

MODELLING OF THE DYNAMIC BEHAVIOUR OF A LADDERMILL, A NOVEL CONCEPT TO EXPLOIT WIND ENERGY

J. P. Meijaard¹, W. J. Ockels² and A. L. Schwab¹

¹Laboratory for Engineering Mechanics, Delft University of Technology
Mekelweg 2, NL-2628 CD Delft, The Netherlands

²Faculty of Aerospace Engineering, Delft University of Technology
PO Box 5058, NL-2600 GB Delft, The Netherlands

ABSTRACT

Recently a novel concept, called the laddermill, was brought forward in order to exploit the high energy flux of wind at high altitudes. This device consists of a number of wings connected by cables. A way to model this device is presented, which considers the wings as rigid bodies and the parts of the cables between them as flexible. A special truss element for modelling cables is described. The aerodynamic forces are described as is usual for cables and aircraft. An application to a preliminary design concept for a laddermill is presented.

INTRODUCTION

Because the energy flux of the wind increases considerably with increasing altitude, it has an advantage to place wind turbines as high as possible. A novel invention, named the *laddermill* (patent Netherlands No 1004508, 12 November 1996, inventor W.J. Ockels, registered in the US and the European Common Market) points to a possible way to exploit this energy source. The laddermill (Fig. 1) is a self-supporting system that consists of one or more endless cables connected to a series of lifting bodies, henceforward called wings, with a high lift that move up and a series of wings with low lift that move down. This results in a difference in the tensile forces of the cable parts at the ground, which can drive an energy generator. The difference in lift of the ascending and descending wings is obtained by controlling the angles of attack of the two sets of wings. The device can be designed to reach several levels of altitude and heights up to the tropopause appear to be technically feasible.

The extreme slenderness of the structure makes a thorough dynamic analysis of paramount importance. Concepts from the finite element method are used for the modelling. The cables are modelled by truss elements, while the wings are considered as rigid bodies. The nodal points are chosen in the centres of mass of the bodies. The trusses can have eccentric rigid connections to these nodal points and the influence of sag due to gravity and wind loading are taken into account, which results in a tensile force in the trusses for almost all conditions and a smooth transition from slack to tight conditions. The equations of motion for the wings are formulated with respect to body-fixed reference systems, which follows the common practice in flight dynamics and

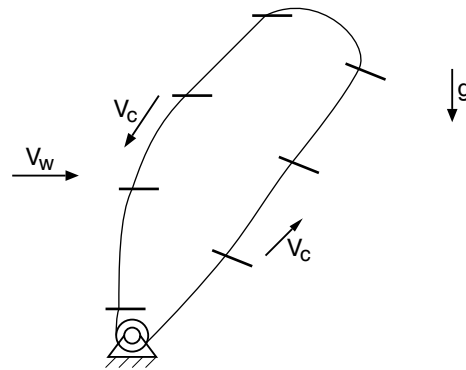


Fig. 1: Laddermill concept.

allows the use of available data for the aerodynamic forces. The equations of motion are integrated by the classic fourth-order Runge-Kutta method.

The formulation has been implemented in two special-purpose computer programmes for the longitudinal in-plane motion and for the complete three-dimensional motion. By exploiting the special nature of the structure, these simulators are far superior in computing speeds than would be possible by making use of general-purpose software.

The following sections describe the modelling of the system and show some results for a preliminary design. Other aspects of the laddermill have been discussed in [1].

MODEL DESCRIPTION

Global frame of reference

It is assumed that the earth is flat and at rest. The origin O of a global frame of reference $Oxyz$ is put at the ground in the vicinity of the point where the cable is veered out or hauled home. The x -axis points in the direction of the nominal wind (“north”), the z -axis points vertically down (“nadir”), and the y -axis is such that an orthogonal right-hand frame of reference is formed (“east”). As an auxiliary quantity the altitude h , $h = -z$, is used.

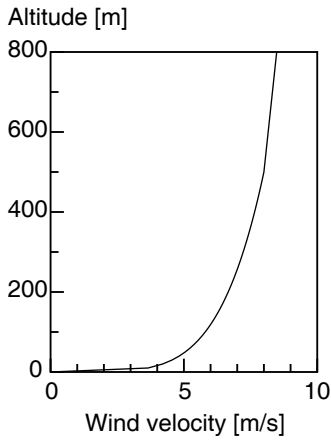


Fig. 2: Average wind velocity profile for the altitude range $0 < h < 800$ m.

The wind velocity can be some general function of time and place. For a first analysis, it suffices to consider only the horizontal mean wind velocity, which is averaged over some short time interval such that the influence of variations due to turbulence or gusts is eliminated. This short-time average horizontal wind velocity as a function of the altitude, $V_w(h)$, is approximated by a profile consisting of a part described by a power law for low altitudes (the atmospheric boundary layer) and a linear part above this layer up to the tropopause as

$$\begin{aligned} V_w(h) &= V_0(h/h_0)^{0.2} \quad (0 < h < h_0), \\ V_w(h) &= V_0 + V_1(h - h_0) \quad (h_0 < h). \end{aligned} \quad (1)$$

Here, h_0 is the thickness of the boundary layer, V_0 is the average wind velocity at the top of this layer, and V_1 is the velocity gradient above this layer. Some typical values are $V_0 = 8$ m/s, $h_0 = 500$ m, $V_1 = 0.0016$ 1/s. Figure 2 shows this profile for $0 < h < 800$ m. The exponent 0.2 was proposed in [2]; other approximate formulas can be found in [3]. For two-dimensional problems, the direction of the wind velocity is assumed to be fixed in the negative x -direction, while for three-dimensional problems, the direction may change as a function of the altitude: for instance, the angle ϕ_s may be given by

$$\phi_s(h) = \phi_s(\infty)[1 - \exp(-h/h_s)], \quad (2)$$

where h_s is some characteristic height for the variation of the direction of the wind.

The mass density of the air as a function of the altitude, $\rho_a(h)$, can be approximated by the barometric altitude formula for constant temperature,

$$\rho_a(h) = \rho_a(0) \exp(-h/H_b), \quad (3)$$

where $H_b = p(0)/(\rho_a(0)g) \approx 8400$ m is the thickness of a uniform atmosphere, or by the value for the standard atmosphere.

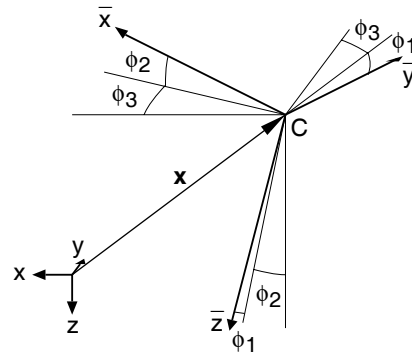


Fig. 3: Position and orientation of a wing. The index p has been omitted in the annotations for the sake of clarity.

Wings

The wings are considered to be rigid. The equations of motion for each wing are formulated with respect to a body-fixed frame $C_p \bar{x}_p \bar{y}_p \bar{z}_p$, where C_p is located in the centre of mass of wing p , the \bar{x}_p -axis points to the direction of the nose of the wing, the \bar{z}_p -axis points to the underside of the wing and the \bar{y}_p -axis points to the right. The $C_p \bar{x}_p \bar{z}_p$ -plane is a plane of symmetry for the body. The position of the centre of mass with respect to the global frame of reference is denoted by the vector \mathbf{x}_p , while the orientation is described by the customary modified Euler angles with order of rotation 3-2-1, with the yaw angle (compass angle) ϕ_{3p} , the pitch angle (inclination) ϕ_{2p} and the roll (bank) angle ϕ_{1p} (Fig. 3).

The equations of motion are

$$\begin{aligned} m_p(\dot{\mathbf{v}}_p + \boldsymbol{\omega}_p \times \mathbf{v}_p) &= \mathbf{f}_p, \\ \mathbf{J}_p \dot{\boldsymbol{\omega}}_p + \boldsymbol{\omega}_p \times \mathbf{J}_p \boldsymbol{\omega}_p &= \mathbf{M}_p. \end{aligned} \quad (4)$$

Here, \mathbf{f}_p and \mathbf{M}_p are the total applied force vector and moment vector with respect to the body-fixed frame of reference; m_p is the mass and \mathbf{J}_p is the inertia tensor. \mathbf{v}_p and $\boldsymbol{\omega}_p$ are the velocity of the centre of gravity and the angular velocity expressed in components with respect to the body-fixed frame of reference. Besides the equations of motion, the kinematic differential equations relate the rates of the position and orientation variables to the velocity variables as

$$\dot{\mathbf{x}}_p = \mathbf{R}_p(\phi_{1p}, \phi_{2p}, \phi_{3p}) \mathbf{v}_p \quad (5)$$

and

$$\begin{pmatrix} \dot{\phi}_{1p} \\ \dot{\phi}_{2p} \\ \dot{\phi}_{3p} \end{pmatrix} = \mathbf{A}_p(\phi_{1p}, \phi_{2p}, \phi_{3p}) \boldsymbol{\omega}_p. \quad (6)$$

The precise form of the rotation matrix \mathbf{R}_p and the matrix \mathbf{A}_p , together with other details, can be found in [4].

The applied forces and moments consist of gravity forces, which act in the direction of the global z -axis, the forces exerted by the cables on the bodies, and the aerodynamic forces from the surrounding air. The last kind of forces are derived from their quasistationary values and expressed in components with respect to a body-fixed frame of reference. The longitudinal forces in the plane of symmetry and the

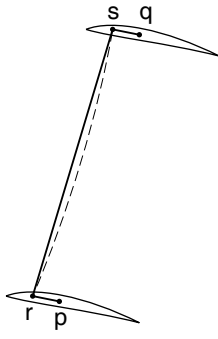


Fig. 4: Cable element with eccentric connections.

lateral forces are assumed to be decoupled. The longitudinal forces depend on the angle of attack and its rate in a non-linear way. The lateral forces are linearized with respect to side slip angle, yaw rate and roll rate, where the coefficients depend on the angle of attack.

Cable elements

Kinematics. A segment of the cable between two wings which are identified by the nodes p and q is modelled by a truss element with eccentric attachment points, which are called r and s (see Fig. 4). For a refined analysis this segment can be subdivided into a number of such elements, without wings or eccentricities at intermediate points. The eccentricities are given by \mathbf{a}_p and \mathbf{a}_q , expressed in components with respect to body-fixed frames of reference. If the cables are attached to identical wings in a single point, then $\mathbf{a}_p = \mathbf{a}_q$.

As a measure for the axial deformation of the cable element the change in length between the attachment points as compared to the nominal unstretched length of the piece of cable is chosen. If we introduce the auxiliary vector between the points of attachment \mathbf{l} and its length l as

$$\begin{aligned} \mathbf{l} &= \mathbf{x}_s - \mathbf{x}_r = \mathbf{x}_q + \mathbf{R}_q \mathbf{a}_q - \mathbf{x}_p - \mathbf{R}_p \mathbf{a}_p, \\ l &= \|\mathbf{l}\| = \sqrt{\mathbf{l} \cdot \mathbf{l}}, \end{aligned} \quad (7)$$

this deformation ε is

$$\varepsilon = l - l_0, \quad (8)$$

where l_0 is the undeformed nominal length of the cable element. The rate of deformation, the derivative of ε with respect to time, is given by

$$\dot{\varepsilon} = \frac{\mathbf{l} \cdot \dot{\mathbf{l}}}{l} = \mathbf{e}_{\bar{x}} \cdot \dot{\mathbf{l}}. \quad (9)$$

Here $\mathbf{e}_{\bar{x}} = \mathbf{l}/l$ is a unit vector in the direction of the vector \mathbf{l} and

$$\dot{\mathbf{l}} = \dot{\mathbf{x}}_s - \dot{\mathbf{x}}_r = \mathbf{R}_q (\mathbf{v}_q + \boldsymbol{\omega}_q \times \mathbf{a}_q) - \mathbf{R}_p (\mathbf{v}_p + \boldsymbol{\omega}_p \times \mathbf{a}_p). \quad (10)$$

Mass description. If there are no eccentricities and the velocities of the nodes are described with respect to a global

inertial frame of reference, the mass matrix for a truss element is given by

$$\mathbf{M}_{0e} = \frac{m_e}{6} \begin{pmatrix} 2\mathbf{I} & \mathbf{I} \\ \mathbf{I} & 2\mathbf{I} \end{pmatrix}, \quad (11)$$

where m_e is the mass of the element and \mathbf{I} is the three-dimensional identity matrix. Because of the eccentricities and because nodal velocities are given with respect to body-fixed frames of reference, this mass matrix has to be transformed. The connection of the velocity quantities of the nodes and the velocities of the points of attachment of the cables is given by a transformation matrix \mathbf{T} as

$$\begin{pmatrix} \dot{\mathbf{x}}_r \\ \dot{\mathbf{x}}_s \end{pmatrix} = \mathbf{T} \begin{pmatrix} \mathbf{v}_p \\ \boldsymbol{\omega}_p \\ \mathbf{v}_q \\ \boldsymbol{\omega}_q \end{pmatrix}, \quad (12)$$

$$\mathbf{T} = \begin{pmatrix} \mathbf{R}_p & -\mathbf{R}_p \tilde{\mathbf{a}}_p & \mathbf{0} & \mathbf{0} \\ \mathbf{0} & \mathbf{0} & \mathbf{R}_q & -\mathbf{R}_q \tilde{\mathbf{a}}_q \end{pmatrix}. \quad (13)$$

Here $\dot{\mathbf{x}}_r$ and $\dot{\mathbf{x}}_s$ are the velocities at the attachment points of the bodies p and q respectively, and $\tilde{\mathbf{a}}$ is the antisymmetric matrix associated with the vector \mathbf{a} such that $\mathbf{a} \times \mathbf{b} = \tilde{\mathbf{a}} \mathbf{b}$ for any vector \mathbf{b} . With this, the transformed mass matrix becomes

$$\mathbf{M}_e = \mathbf{T}^T \mathbf{M}_{0e} \mathbf{T}. \quad (14)$$

In addition to the inertia terms given by the mass matrix multiplied by the time derivatives of the velocity quantities, there are inertia terms that are homogeneous quadratic functions in the velocity variables, \mathbf{h}_e , which are obtained from the time derivative of the matrix \mathbf{T} as

$$-\mathbf{h}_e = \mathbf{T}^T \mathbf{M}_{0e} \begin{pmatrix} \mathbf{R}_p [\boldsymbol{\omega}_p \times (\mathbf{v}_p + \boldsymbol{\omega}_p \times \mathbf{a}_p)] \\ \mathbf{R}_q [\boldsymbol{\omega}_q \times (\mathbf{v}_q + \boldsymbol{\omega}_q \times \mathbf{a}_q)] \end{pmatrix}. \quad (15)$$

Stress-strain relation. In principle it is feasible to use the customary linear relation between stress and strain for the truss elements. However, because we intend to use only one element between two wings, or at least a number as small as possible, and intend to prevent the occurrence of compressive forces in the elements, which cannot exist in ideal cables, a non-linear stress-strain relation is proposed that takes into account the sag of the pieces of cable caused by gravity and wind load. Usually a constant distributed load is assumed over the length of the element, but because the aerodynamic load on the cables may vary over its length, and an incidentally nearly zero lateral load on the cable has to be prevented, a linearly varying load is assumed in the lateral directions of the cable. For the calculation of the stress-strain relation, a local system of coordinates with origin at the attachment point r , \bar{x} -direction pointing towards the attachment point s and the \bar{y} and \bar{z} -direction perpendicular to this line and to each other. The linear approximation for the distributed load in these directions, denoted by p_y and p_z , yields lateral deflections which, to first order, have to satisfy the equations

$$\begin{aligned} p_y &= p_{yr}(1 - \xi) + p_{ys}\xi = -\sigma v'', \\ p_z &= p_{zr}(1 - \xi) + p_{zs}\xi = -\sigma w'', \end{aligned} \quad (16)$$

where $\xi = \bar{x}/l$, $0 \leq \xi \leq 1$, is the non-dimensional coordinate along the \bar{x} -axis; p_{yr} , p_{ys} , p_{zr} and p_{zs} are the values of the lateral loads at the points of attachment r and s ; σ is the desired tensile force in the cable, v and w are the lateral deflections and a prime denotes a derivative with respect to the \bar{x} -coordinate. The contribution of the inertia terms to the lateral deflection is excluded, because these are not known initially. The solutions of these equations are given by

$$\begin{aligned}\sigma v &= p_{yr}l^2\left(\frac{1}{3}\xi - \frac{1}{2}\xi^2 + \frac{1}{6}\xi^3\right) + p_{ys}l^2\left(\frac{1}{6}\xi - \frac{1}{6}\xi^3\right), \\ \sigma w &= p_{zr}l^2\left(\frac{1}{3}\xi - \frac{1}{2}\xi^2 + \frac{1}{6}\xi^3\right) + p_{zs}l^2\left(\frac{1}{6}\xi - \frac{1}{6}\xi^3\right).\end{aligned}\quad (17)$$

These deflections give a contribution to the true elongation, measured along the deflected cable, the principal term of which is

$$\begin{aligned}\int_0^1 \frac{1}{2}[(v')^2 + (w')^2]l d\xi &= \frac{\varepsilon_p}{\sigma^2} = \\ \frac{1}{\sigma^2} \left(\frac{1}{90}p_{yr}^2l^3 + \frac{7}{360}p_{yr}p_{ys}l^3 + \frac{1}{90}p_{ys}^2l^3 \right) &+ \\ \frac{1}{\sigma^2} \left(\frac{1}{90}p_{zr}^2l^3 + \frac{7}{360}p_{zr}p_{zs}l^3 + \frac{1}{90}p_{zs}^2l^3 \right).\end{aligned}\quad (18)$$

The relation between the true elongation and the tensile force is now given by the usual linear relation as

$$\sigma = \frac{EA}{l_0}(\varepsilon + \frac{\varepsilon_p}{\sigma^2}) + \frac{DA}{l_0}\varepsilon. \quad (19)$$

Here A is the surface of the cross-section of the cable, E is the effective modulus of elasticity and D is the corresponding damping modulus in the Voigt model, where it is assumed that the lateral deflection has no influence on the damping. This assumption is allowed if the damping is small or neglected.

The above cubic equation can be solved exactly, but preference is given to the iterative Newton-Raphson method, which is more robust and converges fast, especially if the contribution of the lateral deflection is small. In this method a zero of the scalar function

$$f_\sigma(\sigma) = \sigma^3 - \frac{EA\varepsilon + DA\varepsilon}{l_0}\sigma^2 - \frac{EA\varepsilon_p}{l_0} \quad (20)$$

is sought. As an initial guess for the solution,

$$\sigma^{(0)} = \max\left(\frac{EA\varepsilon + DA\varepsilon}{l_0}, \sqrt[3]{\frac{EA\varepsilon_p}{l_0}}\right) \quad (21)$$

is chosen. From a present approximation $\sigma^{(i)}$, a subsequent approximation $\sigma^{(i+1)}$ is found as

$$\sigma^{(i+1)} = \sigma^{(i)} - \frac{f_\sigma(\sigma^{(i)})}{df_\sigma/d\sigma}, \quad (22)$$

until convergence has been achieved. The iteration process converges if the two points of attachment do not coincide ($l > 0$) and the lateral load is unequal to zero ($\varepsilon_p > 0$).

The tensile force σ gives a contribution to the global force vector of the system of $-\mathbf{D}_e^T \sigma$, where the difference matrix \mathbf{D}_e has been introduced, $\mathbf{D}_e = (-\mathbf{e}_{\bar{x}}^T \quad \mathbf{e}_{\bar{x}}^T)\mathbf{T}$.

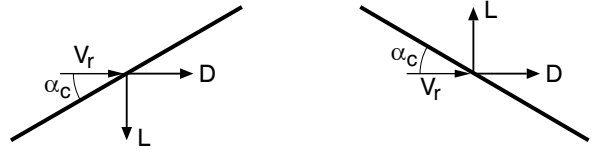


Fig. 5: Aerodynamic loads on the cables for two cases.

Loads on the cable. The load on the cable consists of a part due to gravity, which points to the global z -direction and has a magnitude of $\rho_c Ag$ per unit of undeformed length, where ρ_c is the mass density of the cable, and g is the acceleration of gravity. Another part is due to the relative flow of the surrounding air, which yields a drag force in the direction of the relative wind velocity and a lift force perpendicular to this direction in the plane of the relative wind velocity and the tangent to the cable. For the calculation of the aerodynamic load the influence of the sag as described above is neglected. The drag D and the lift L per unit of length are given by

$$D = \frac{1}{2}C_d\rho_a V_r^2 d_c, \quad L = \frac{1}{2}C_l\rho_a V_r^2 d_c, \quad (23)$$

where V_r is the magnitude of the relative wind velocity and d_c is the diameter of the cable. The drag and lift coefficients C_d and C_l are taken from [5] to be

$$\begin{aligned}C_d &= C_{N0} \sin^3 \alpha_c + C_{T0}, \\ C_l &= C_{N0} \sin^2 \alpha_c \cos \alpha_c,\end{aligned}\quad (24)$$

where the angle of attack α_c is taken in the interval $[0, \pi)$ and the lift has the corresponding direction (Fig. 5). Except for extreme cases, the Reynolds number is below the critical turbulent value, which is of the order 10^5 , and the values $C_{N0} = 1.1$, $C_{T0} = 0.02$ are chosen.

The distributed applied load is replaced by statically equivalent nodal forces at the nodes.

Boundary conditions

Two nodal points are fixed at the generator. The motion of the cable is taken into account by changing the undeformed length l_0 of the first and last cable element at the rate of the cable speed V_c . This changes the constitutive relation and the total mass of the element accordingly. Initially the length of the first element is $\frac{1}{10}l_0$ and the length of the last element is $\frac{11}{10}l_0$. If the cable has moved a distance l_0 , a wing is taken off from the hauled part of the cable and a wing is added on the veered part of the cable. The two adjacent elements on the hauled part are combined into a single element and the first element of the veered part is split into two elements, with the new wing attached to their common node. The new coordinates and velocities of this body are obtained from a linear interpolation.

System equations of motion

The equations of motion for the whole system are obtained by a standard finite element assembly process from the contributions of each body and element. The global mass matrix consists of contributions from the wings and from the

elements. The global force vector is composed of velocity dependent mass terms \mathbf{h} , external forces \mathbf{f} and element forces $-\mathbf{D}^T \boldsymbol{\sigma}$. With these, the equations of motion become

$$\mathbf{M}\dot{\mathbf{v}} = \mathbf{f} + \mathbf{h} - \mathbf{D}^T \boldsymbol{\sigma}. \quad (25)$$

All velocity variables of the nodes are grouped together in the vector \mathbf{v} . The mass matrix is position as well as time dependent, so the equations of motion have to be solved for the rates of the velocity variables in each function evaluation of the numerical integration scheme. Because of the band structure of the matrix, this involves a limited amount of work.

In addition to the equations of motion, the kinematic differential equations that relate the rates of the position variables to the velocity variables have to be integrated in time.

For the numerical integration of the full set of first-order differential equations, the classic explicit fourth-order Runge-Kutta method [6] with a fixed time step is used. It has been shown in [7] that this method is suitable for mechanical systems of the kind considered here.

Implementation.

The model has been implemented into two special purpose computer programmes written in the language Fortran-77, one for the two-dimensional case, and one for the three-dimensional case. For the two-dimensional case, the out of plane motion is not needed and the equations are simplified accordingly.

EXAMPLES OF APPLICATION

System configuration

A model is considered which consists of 103 nodes, with 101 lifting bodies separated by pieces of cables of length 70 m, so the maximal height that can be reached is about 3500 m. The lifting bodies consist of a pair of wings with a splitting, to which tail booms are connected which have a horizontal and a vertical tail surface. The angle of attack can be controlled by turning the horizontal tail surfaces. The main wings have an area of 54 m^2 , a span of 20 m, and a weight of 54 kg. The distance between the centre of gravity and the aerodynamic centre of the main wing is 0.75 m, while the distance to the point of attachment, that is, the magnitude of the eccentricity of the cable elements, is 1.50 m, while the tail booms are 5 m long. The diameter of the cables is 2.5 cm, and the weight of the pieces of cable is 21 kg. The parameters for the wind profile are $V_0 = 8 \text{ m/s}$, $V_1 = 0.0016 \text{ 1/s}$, $h_0 = 50 \text{ m}$. The laddermill is placed at a height of 50 m.

Two-dimensional results

For the in-plane motion, the final shapes that the device obtains for $V_c = 1 \text{ m/s}$ and $V_c = 5 \text{ m/s}$ are shown in Fig. 6. One should note that due to the removing and attaching of wings near the ground, the resulting motion is periodic, and

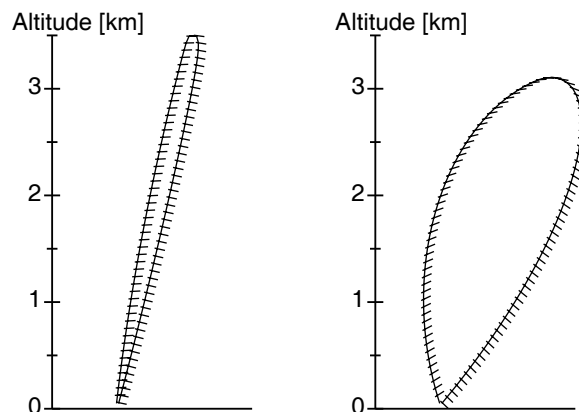


Fig. 6: Stationary shape of the mill for the cable speed $V_c = 1 \text{ m/s}$ (left diagram) and for $V_c = 5 \text{ m/s}$ (right diagram).

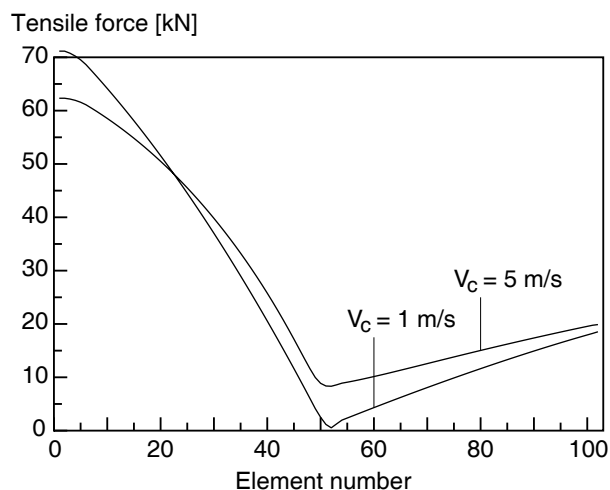


Fig. 7: Tensile force in the elements for the two cases shown in Fig. 6.

periodic variations of the shape occur. For low cable velocities, the ascending and descending part are almost parallel, and danger of mutual collisions is present. For larger cable velocities, the loop widens, because the difference in the direction of the relative wind velocity for the two part increases. Figure 7 shows the tensile force in the cable. The tensile force is smallest near the top, which value increases as the loop widens. The difference in tensile force between the first and last element drives the generator. A fair estimate of the power is obtained by the product of this difference and the cable speed. In the considered case with a moderate wind, this power is of the order of 200 kW, where it has to be noted that the configuration has not been optimized for a maximal energy yield.

If the tail surface is sufficiently large, the in-plane motion appears to be remarkably stable for disturbances. If the distribution of the wind velocity or the cable speed change, the mill comes to a new stationary motion after some transient motions.

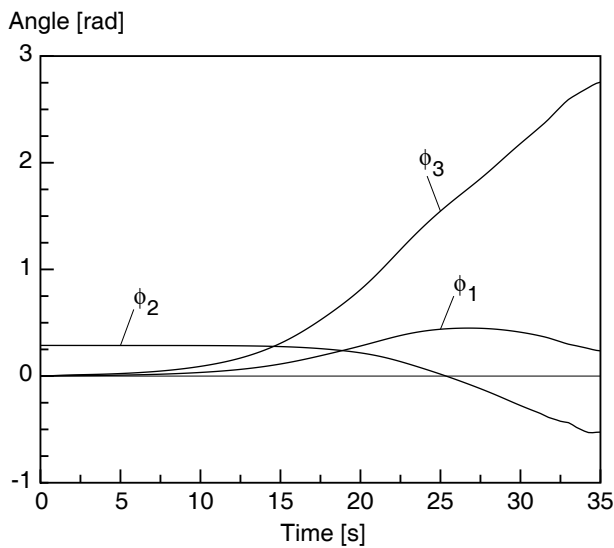


Fig. 8: Rotational motion of node 40 for a disturbance of 0.01 rad in the direction of the wind; $V_c = 2$ m/s.

Three-dimensional results

As a test, in-plane motions were calculated with the programme for two-dimensional motions as well as the programme for three-dimensional motions. The results were almost identical.

If the stationary in-plane motion is disturbed, the resulting motion appears to be unstable. As an example, the influence of a small change in the direction of the wind on the orientation of the wing at node number 40 (in the ascending part close to the top) is shown in Fig. 8. The wing yaws over a large angle before the calculations breaks down after some 40 seconds. This break-down of the programme is caused by the chosen fixed step size in the integration method; with a smaller step size, the simulation could be continued longer. Furthermore, the angles of attack, the side-slip angle and the yaw and roll rate come in a range for which the aerodynamic data for the wings are no longer accurate.

The instability of the out-of-plane motion for a glider fixed to a cable has been observed in several other investigations, among others [8, 9], even if the glider would fly in a stable way without cable. This instability appears to be caused by the splitting of the multiple zero eigenvalues. For the in-plane motion, this multiplicity is two; if the eigenvalues split in a direction along the imaginary axis, stability can be maintained. For the out-of-plane motion, the multiplicity is also two. It appears that for the perturbation of finite size an interaction with two other small eigenvalues make the system resemble a system with a zero eigenvalue with multiplicity four, which is generically unstable for small perturbations.

CONCLUSIONS

A way to model the laddermill concept has been described. This model has been implemented in two computer programmes, which make possible an efficient and robust simu-

lation, almost in real time, of the motion of design concepts. A special way to model the tensile force in the cables, in order to avoid a sharp transition between slack and tight conditions, has proved to be successful. The changing length of the first and last cable segments could be easily incorporated by changing the nominal length of the corresponding truss elements. By formulating the equations of motion of the wings with respect to a body-fixed frame of reference, use could be made of standard aerodynamic coefficients.

The results of simulations for a preliminary design showed that the in-plane dynamic behaviour could be made satisfactory. The lateral motion, however, showed instability for the proposed wing configuration. The possibility of improving the stability by a change of the design or by adding additional controls will be considered in future.

REFERENCES

- [1] W. J. Ockels and H. J. van Grol, "Laddermill, a novel concept to exploit the energy in the airspace," paper presented at the 1999 European Wind Energy Conference and Exhibition, Nice.
- [2] G. Hellmann, "Über die Bewegung der Luft in den untersten Schichten der Atmosphäre," *Meteorologische Zeitschrift* **34** (1917), pp. 273–285.
- [3] E. Simiu and R. H. Scanlan, *Wind Effects on Structures, Fundamentals and Applications to Design* (third edition), John Wiley & Sons, New York, 1996.
- [4] J.-L. Boiffier, *The Dynamics of Flight, the Equations*, John Wiley & Sons, Chichester, 1998.
- [5] S. F. Hoerner, *Fluid-Dynamic Drag, Practical Information on Aerodynamic Drag and Hydrodynamic Resistance*, Hoerner Fluid Dynamics, Albuquerque NM, 1965.
- [6] L. F. Shampine, *Numerical Solution of Ordinary Differential Equations*, Chapman & Hall, New York/London, 1994.
- [7] J. P. Meijaard, "A comparison of numerical integration methods with a view to fast simulation of mechanical dynamical systems," in *Real-Time Integration Methods for Mechanical System Simulation*, Springer, Berlin/Heidelberg, 1991, pp. 329–343.
- [8] L. W. Bryant, W. S. Brown and N. E. Sweeting, *Collected Researches on the Stability of Kites and Towed Gliders*, Aeronautical Research Council Reports and Memoranda No 2303, His Majesty's Stationery Office, London, 1950.
- [9] J. D. DeLaurier, *A Stability Analysis of Cable-Body Systems Totally Immersed in a Fluid Stream*, NASA Contractor Report CR-2021, NASA, Washington DC, 1972.